Available online at www.sciencedirect.com
ScienceDirect
Ceramics International 34 (2008) 1327–1333
CERAMICS INTERNATIONAL
www.elsevier.com/locate/ceramint

Influence of erbia or europia doping on crystal structure and microstructure of ceria–zirconia (CZ) solid solutions

Stefano Maschio [a,*], Eleonora Aneggi [a], Alessandro Trovarelli [a], Valter Sergo [b]

[a] Università di Udine, Dipartimento di Scienze e Tecnologie Chimiche, Via del Cotonificio 108, 33100 Udine, Italy
[b] Università di Trieste, Dipartimento dei Materiali e delle Risorse Naturali, Via A. Valerio 2, 34127 Trieste, Italy

Received 2 January 2007; received in revised form 1 March 2007; accepted 17 March 2007
Available online 10 April 2007

Abstract

In this study we have prepared three zirconia–ceria compositions, namely 12, 50 and 80 mole% CeO_2. Along with each pure ceria–zirconia composition we have prepared two parallel erbia- or europia-doped materials in which 0.5 mole% of each of the two starting oxides is replaced by 1 mole erbia or europia.

We observed that the microstructures of CZ12 samples are fairly homogeneous in grain size distribution, while those doped with erbia or europia present large as well as small grains, but smaller average size than pure CZ12.

Pure CZ50 solid solution showed the presence of two tetragonal phases whereas CZ50-Er and CZ50-Eu show the presence of two phases if sintered below 1450 °C, but only one above 1450 °C. The grains of CZ50 and CZ50-Er have wavy borders and faceting, whereas those of CZ50-Eu have rounded borders and faceting is not greatly displayed.

CZ80 series showed the cubic fluorite structure for any sintering cycle, but the addition of europia reduces the grain size with respect to the pure CZ80 and to the parallel erbia-doped solution.

Keywords: A. Sintering; B. Microstructure-final; D. ZrO_2; D. CeO_2; Crystal phases

1. Introduction

Cerium oxide has been widely studied in recent years because of its potential usefulness for catalytic applications. Cerium oxide is currently being used as a promoter in the automotive three-way catalysts owing to its ability to undergo rapid reduction/oxidation cycles by shifting between CeO_2 under oxidizing conditions and Ce_2O_3 under reducing conditions, respectively. The capabilities of the redox couple Ce^{4+}–Ce^{3+} are strongly enhanced if other elements are introduced into the CeO_2 lattice. In particular, it has been reported that ceria–zirconia (CeO_2/ZrO_2) mixed oxides show enhanced thermal, redox and catalytic properties compared to pure CeO_2 [1–8].

The ceria–zirconia system has been studied as an alternative to the more investigated yttria-zirconia also for the presence of two tetragonal phases: one, usually called TZ°, exists for compositions ranging from 7.5 to 16 mole% CeO_2; the other, called TZ′, is stable between 16 and 50 mole% CeO_2. TZ° can transform to the monoclinic polymorph under an applied stress field, thus raising the materials toughness. TZ′ does not transform as it is derived from the high temperature cubic phase via an appropriate cooling rate, which re-equilibrates the oxygen content, resulting in a displacive transformation to a high ceria content tetragonal phase. For compositions lower than 7.5 mole% CeO_2 the monoclinic phase is stable, whereas fluorite structures are normally detected above 50 mole% CeO_2 [9–16].

The possibility for other rare-earth oxides to form solid solutions with zirconia is documented [17–19], and among these, erbia, Er_2O_3 and europia, Eu_2O_3 [20–25]. Even in very limited amounts, the addition of other oxides to ceria–zirconia solid solutions may cause significant modifications in the crystal structure and microstructure of the resulting materials.

* Corresponding author. Tel.: +39 0432 558877; fax: +39 0432 558803.
E-mail addresses: stef.maschio@uniud.it (S. Maschio), Eleonora.aneggi@uniud.it (E. Aneggi), trovarelli@uniud.it (A. Trovarelli), sergo@units.it (V. Sergo).

0272-8842/$34.00
doi:10.1016/j.ceramint.2007.03.006

For example, small silica addition could lead to the formation of interlocking grain boundaries [26].

In this research we have prepared three zirconia–ceria compositions, namely 12, 50 and 80 mole% CeO_2. The first falls in the TZ° range, the second in the bi-phase TZ′/fluorite-type field, the third where only the fluorite-type structure is normally detected. Along with each pure ceria–zirconia composition we have prepared two parallel erbia- or europia-doped materials in which 0.5 mole% of each of the two starting oxides (namely CeO_2 and ZrO_2) is replaced by 1 mole of erbia or europia. The ionic radius of Zr^{4+} is 0.84 Å, that of Ce^{4+} is 0.97 Å, the one of Er^{3+} is 1.00 Å whereas that of Eu^{3+} is 1.07 Å [27].

2. Experimental procedure

The first step of powder preparation was performed by coprecipitation. Starting materials used were: $ZrOCl_2{\cdot}8H_2O$ (99.0% Aldrich Chem.), $Ce(NO_3)_3{\cdot}6H_2O$ (99.9% Aldrich Chem.), $Er(NO_3)_3{\cdot}5H_2O$ (99.9% Aldrich Chem.) and $Eu(NO_3)_3{\cdot}5H_2O$ (99.9% Aldrich Chem.). The required proportions of precursors were dissolved into distilled water to give 0.5 M solutions. Table 1 presents the compositions of the samples prepared, as well as the abbreviation used throughout the paper to define them. Zirconium oxychloride octahydrate is a relatively cheap precursor for zirconia, whereas for the other species nitrates were preferred to chlorides because nitrogen compounds can be eliminated more easily than chlorides from the coprecipitated products.

The solutions were poured drop wise while stirring into concentrated ammonia (28 mass%) at room temperature. After coprecipitation the products were maintained under stirring for 2 h to allow the complete reaction of the components. Co-precipitated products were washed several times with deionized water and then with an acetone–toluene–acetone sequence [28]. The resulting powders were heated at 80 °C in an oven and sieved through a 63 μm sieve. After drying, powders were attrition milled for 1 h using isopropanol as dispersing liquid in a plastic container with zirconia/yttria (3 mole%) spheres at 300 cycle/min, as recently suggested [29].

Simultaneous thermal analysis (STA) was performed (Netzsch STA) with a heating rate of 10 °C/min up to a temperature of 1250 °C; the STA analysis was used to select the calcination procedure of 2 h at 650 °C. After the calcinations, powders were re-attrition milled using 2-buthanol as dispersing medium (2-buthanol has a lower vapour pressure than isopropanol, so that it is not necessary to introduce additional alcohol during the milling process).

Table 1
Composition of the samples and corresponding abbreviations used in the present paper

Sample composition	Abbreviation used in the present paper
$(ZrO_2)_{0.88}(CeO_2)_{0.12}O_2$	CZ12
$(ZrO_2)_{0.5}(CeO_2)_{0.5}\ O_2$	CZ50
$(ZrO_2)_{0.2}(CeO_2)_{0.8}O_2$	CZ80
$(ZrO_2)_{0.875}(CeO_2)_{0.115}(Er_2O_3)_{0.01}O_2$	CZ12-Er
$(ZrO_2)_{0.875}(CeO_2)_{0.115}(Eu_2O_3)_{0.01}O_2$	CZ12-Eu
$(ZrO_2)_{0.495}(CeO_2)_{0.495}(Er_2O_3)_{0.01}O_2$	CZ50-Er
$(ZrO_2)_{0.495}(CeO_2)_{0.495}(Eu_2O_3)_{0.01}O_2$	CZ50-Eu
$(ZrO_2)_{0.195}(CeO_2)_{0.795}(Er_2O_3)_{0.01}O_2$	CZ 80-Er
$(ZrO_2)_{0.195}(CeO_2)_{0.795}(Eu_2O_3)_{0.01}O_2$	CZ80-Eu

After drying and sieving, powders were uniaxially pressed at 30 MPa to give cylinders (8 mm D, 25 mm h), which were then isostatically pressed at 300 MPa. Sintering was performed in air within a $MoSi_2$ heated muffle at 1450 and 1550 °C for various times with heating and cooling rates of 10 °C/min.

The apparent density of the sintered bodies was evaluated by the Archimede's method and relative densities were determined assuming 6.23, 6.69 and 6.95 g/cm^3 as theoretical densities for the CZ12, CZ50 and CZ80 series, respectively. For this measures the presence of erbia or europia was neglected.

The crystalline phases of the different compositions were investigated by X-ray diffraction (XRD). XRD patterns were recorded on a Philips X'Pert diffractometer operated at 40 kV and 40 mA using nickel-filtered Cu Kα radiation. Spectra were collected using a step size of 0.02° and a counting time of 40 s per angular abscissa in the range 20–145°. The Philips X'Pert HighScore software was used for phase identification. The mean crystalline size was estimated from the full width at the half maximum (FWHM) of the X-ray diffraction peak using the Scherrer equation [30] with a correction for instrument line broadening. Rietveld refinement [31] of XRD patterns were performed by means of GSAS-EXPGUI program [32,33]. The accuracy of these values was estimated by comparing our measurements against the values of the lattice constant, assuming Vegard's law [34].

Microstructures were examined, on the as fired materials, by an Assing Stereoscan scanning electron microscope (SEM) and the average grain size was determined by the lineal intercept method without correction for grain shape.

3. Results and discussion

Simultaneous thermal analysis (STA) of the powders did not show any appreciable difference. Heating and phase crystallization occurred at low temperature concurrently with a weight loss which ended at 550 °C for all compositions. Consequently, coprecipitated, attrition-milled, dried powders were calcined for 2 h at 650 °C in order to ensure that no organic compounds remained entrapped in the powders particles.

3.1. Low ceria content

Powders of composition CZ12, CZ12-Er and CZ12-Eu were tetragonal after calcination, and the attrition milling procedure only partly transformed this phase into monoclinic (less that 10 vol.%). The presence of erbia/europia shifts the XRD peaks towards lower degree with respect to the pure CZ12, indicating an enlargement of the tetragonal original cell. The increase of the cell volume is compensated by the higher molar weight of the solutions and, hence, the theoretical values of the densities remain practically unchanged with respect to that of the CZ12. The sintering tests demonstrated that fired samples reach high

Table 2
Relative densities of the fired samples as a function of the sintering cycle

Sintering cycle	CZ12	CZ12-Er	CZ12-Eu	CZ50	CZ50-Er	CZ50-Eu	CZ80	CZ80-Er	CZ80-Eu
1450, 1 h	95.5	95	94.5	93.5[a]	94.8	93.8[a]	95	93.7[a]	94.1
1450, 2 h	97	97.5	96.5	95.8	95.9	95.3	95.9	96	95.6
1550, 1 h	99	99.1	97.4	96.7	98	98.2	96.9	97.1	98.3
1550, 2 h	99.7	99.8	99.5	99.6	99.4	99.5	99.4	99.6	99.7

[a] Before the density measurement the free surface of the sample was previously sealed with paraffin.

density after 2 h at 1450 or after 1 h at 1550 °C (Table 2). In all the samples sintered for less than 2 h at 1550 °C only tetragonal phase was present (Table 3), while specimens sintered for 2 h at 1550 °C showed a very low amount of the monoclinic (<5 vol.%), likely due to the spontaneous tetragonal-to-monoclinic transformation of the larger grains. We have also observed that CZ12 samples exhibit fairly homogeneous grain size, while compositions containing erbia or europia show a greater variation in grain dimensions (Fig. 1a–c). Fig. 1a–c also shows that the largest grains of all these three materials have dimension around 2.5 μm; this number can be assumed as the critical grain size above which spontaneous t-m transformation occurs. It follows that materials fired for 2 h or more at 1550 °C contain 2 phases, whereas those fired at lower temperature (1450 °C) or for shorter times contain one phase only.

Fig. 2 shows the trend of the average grain size of CZ12 with and without dopants for a constant temperature of 1550 °C as a function of the time. It appears important to see that at zero time the average grain size of Er- or Eu-doped materials have size below 1 μm and their size is 30% lower than those of CZ12 for any time, that is erbia and europia are very effective grain growth inhibitors. The error associated to the grains measurements is high since all materials contains small as well as large grains. It has been determined as 43% for CZ12, 27% for CZ12-Er and 24% for CZ12-Eu, respectively.

3.2. Intermediate ceria content

CZ50, CZ50-Er and CZ50-Eu powders showed the presence of two phases (Table 3) that were indexed as the TZ′ and TZ″ by the XRD analysis in agreement with other authors [6,35–38] with the TZ″ being an intermediate form between TZ′ and the cubic phase. TZ″ shows no tetragonality, but exhibits an oxygen displacement from ideal fluorite sites and is therefore generally referred as a cubic phase. Attrition milling of the starting powders does not transform such phases, but we have only observed the broadening of the reflection peaks, clearly due to the reduced crystallite size and introduction of strains into the powders.

CZ50 retains these crystal structures after sintering and cooling, for any time, whereas CZ50-Er and CZ50-Eu, for the same firing and cooling conditions do not. In fact, CZ50-Er and CZ50-Eu show the presence of two phases if sintered at 1450 °C, whereas there is only one phase when the sample are fired at 1550 °C, as reported in Table 3.

Fig. 3a–c show the SEM microstructures of the three samples fired for 2 h at 1550 °C. The grains of CZ50-Er

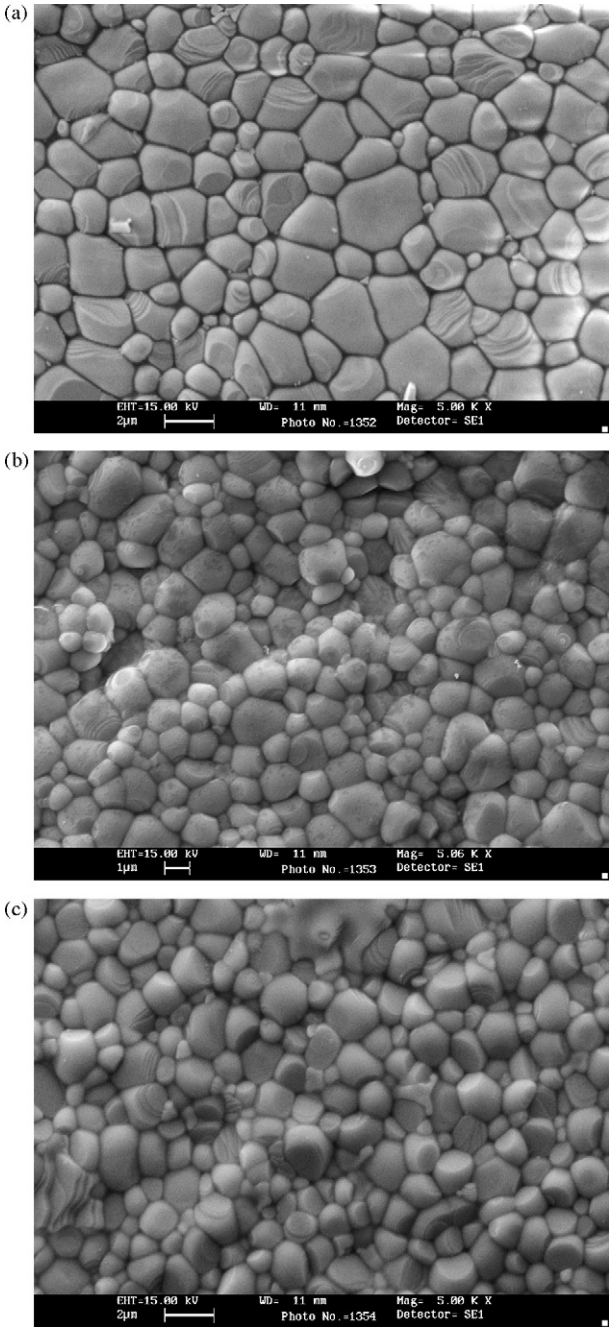

Fig. 1. SEM microstructures of CZ12 materials fired 2 h at 1550 °C. (a) Without any addition; (b) doped with Er; (c) doped with Eu. It must be observed that the software of the SEM automatically generates the marker length which is 1 μm in b and 2 μm in a and c. This is even if the magnification of the three photos is practically the same.

Table 3
Detected phases on the free surface of the sintered specimens

Sintering cycle	CZ12	CZ12-Er	CZ12-Eu	CZ50	CZ50-Er	CZ50-Eu	CZ80	CZ80-Er	CZ80-Eu
1450, 1h	TZ°	TZ°	TZ°	TZ′ + TZ″	TZ′ + TZ″	TZ′ + TZ″	Cub	Cub	Cub
1450, 2h	TZ°	TZ°	TZ°	TZ′ + TZ″	TZ′ + TZ″	TZ′ + TZ″	Cub	Cub	Cub
1550, 1h	TZ°	TZ°	TZ°	TZ′ + TZ″	TZ′	TZ′	Cub	Cub	Cub
1550, 2h	TZ° + m	TZ° + m	TZ° + m	TZ′ + TZ″	TZ′	TZ′	Cub	Cub	Cub

TZ°: transformable tetragonal; m: monoclinic; TZ′: non-transformable tetragonal; TZ″: non transformable tetragonal; Cub: fluorite-type.

(Fig. 3b) have wavy boundaries and grain surface faceting, whereas those of CZ50-Eu (Fig. 3c) have rounded boundaries and grain surface faceting is not greatly displayed. For sake of clarity we use the terms wavy boundaries just to indicate irregular shaped grains and not grains partially sintered. Grains with wavy boundaries were observed by Meriani [26] in similar materials as a result of some silica addition to the pure ceria–zirconia solid solutions. In our materials silica content is negligible even if an undesired, but a limited amount could have been introduced by starting precursors, milling media or solvents that were used for powders preparation. However, all materials were subjected to the same preparation procedure, but only selected compositions show wavy grain boundaries. The thermal treatment to which the materials were subjected can be considered low when compared to that studied by Meriani [26] performed at 1600 °C; in addition, wavy grain boundaries were also observed in samples CZ50 and CZ50-Er fired at 1450 °C for any time, even if the phenomenon is not so pronounced. We tend to assume that the presence of wavy grain boundaries is rather intrinsic to the materials. We might also speculate that the presence of impurities in the powders could facilitate the formation of wavy grain boundaries only in selected compositions, probably indicating no equilibrium resulting from partial sintering. In our materials, it has been observed, that the presence of europia lead to fired samples that are characterized by the presence of rounded and not wavy grain boundaries, independently of the sintering temperature used in the present research. We must therefore suppose that europia reduces the grain borders mobility to a greater extrent than the samples containing erbia or to the pure CZ50 materials.

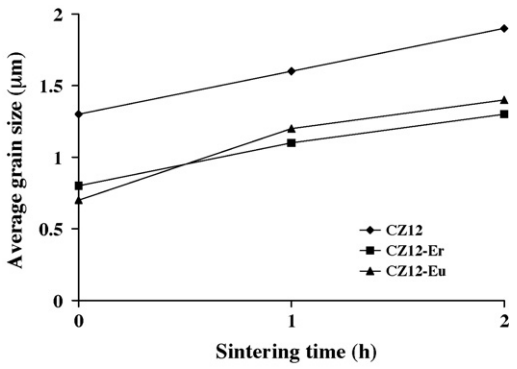

Fig. 2. Grain size vs. sintering time at 1550 °C for the three CZ12 solid solutions.

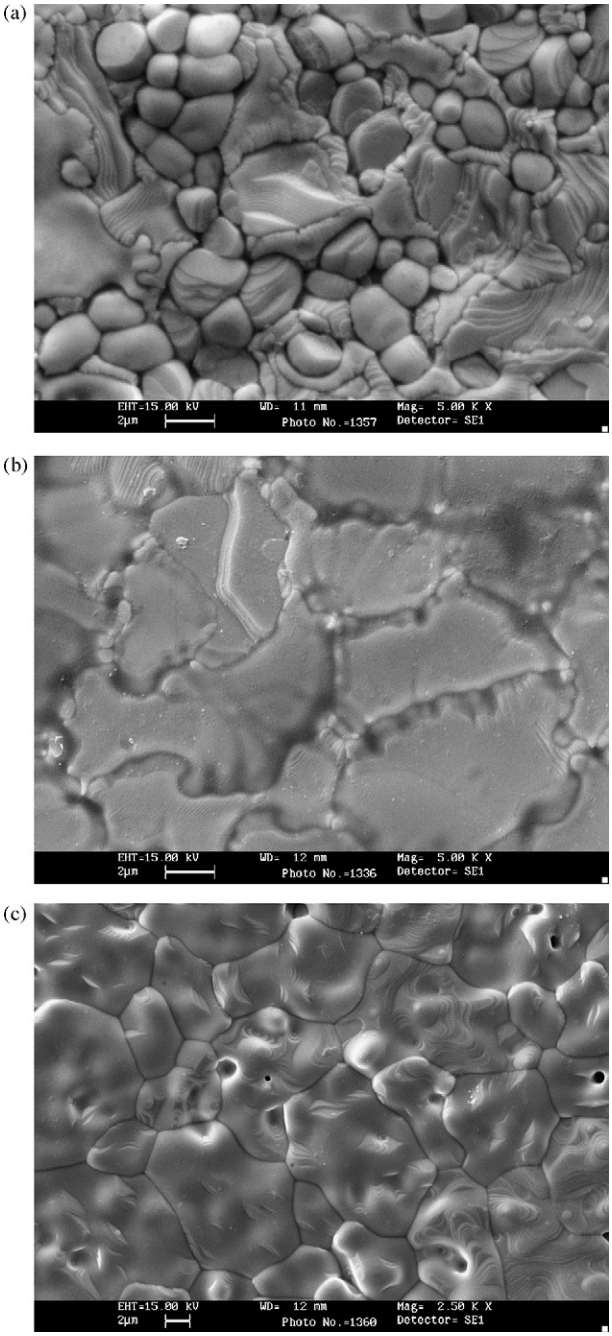

Fig. 3. SEM microstructures of CZ50 materials fired 2 h at 1550 °C. (a) Without any addition; (b) doped with Er; (c) doped with Eu.

3.3. Fluorite-type materials

Powders CZ80, CZ80-Er and CZ80-Eu showed, as expected, the cubic fluorite-type structure. All cubic powders maintained their crystal structure after milling, but the diffraction peaks become wider as a result of the reduction of the crystallite dimensions and strain due to the attrition milling process. Furthermore the materials maintain the fluorite-type structure for any sintering cycle (Table 3). The theoretical density of the materials remains unchanged if erbia or europia are added to the CZ80 solid solution. As in the case of the three CZ12 solid solutions the enlargement of the lattices are compensated by the greater atomic weight of the added elements.

The microstructures are, on the other hand, sensibly different whether the fired materials are doped or not. Fig. 4a–c show the SEM microstructures of the samples sintered 2 h at 1550 °C.

It can be observed that the addition of europia reduces the grain size with respect to the pure CZ80 and to the erbia-doped solution.

Fig. 5 shows the average grain size of CZ80 with and without dopants for a constant temperature of 1550 °C. It can be seen that materials containing europia have smaller average size than pure CZ80 or CZ80-Er. Erbia-doped materials behave as non-doped CZ80 if the hold time at 1550 °C is equal or shorter than 1 h while for longer times the addition of erbia reduces the grain size. It appears also important to observe that at zero hold time the average grain size of Eu-doped materials is 1.7 μm, but that grain growth is fast and, after 2 h, the grains have an average size of 8.2 μm. Erbia-doped materials, after 2 h at 1550 °C, have an average grain size of 10.7 μm. This composition also shows a very large size (5.5 μm) at zero hold time, comparable with that of the non-doped solid solution. Also for these compositions the error associated to the grains measurements is high and it has been determined as 37% for CZ12, 33% for CZ12-Er and 26% for CZ12-Eu, respectively.

In all the CZ80 series, the average grain size is constantly larger than that observed for the CZ12 doped materials due to the high cation mobility which occurs when the solid solutions contain a large amount of ceria [39].

It should also be noted that the observed shape of the grains is different in the Eu-doped materials if compared to the pure CZ80 and to the Er-doped solutions. It can be concluded that europia induces formation and development of regular rounded grains not observed in CZ80 and CZ80-Er where grains are more equiaxed and are often faceted. CZ80-Er presents a very different microstructure at the triple junctions (Fig. 4b): in these locations there appears some protruding or exuded features that, speculatively, we attribute to a grain boundary phase

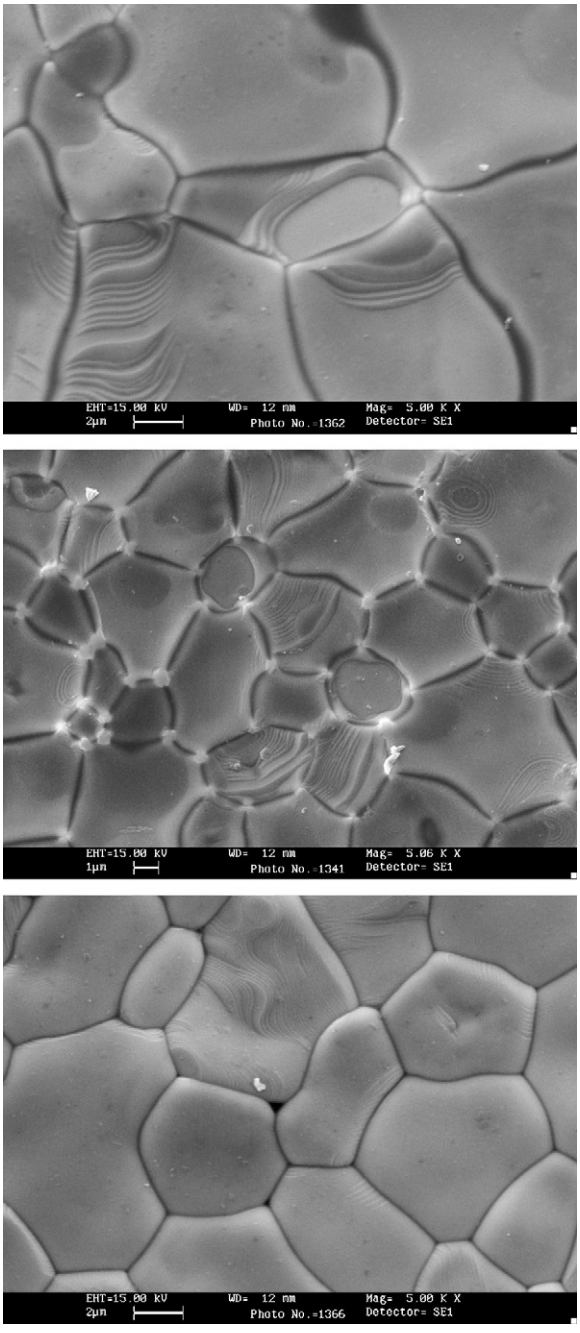

Fig. 4. SEM microstructures of CZ80 materials fired 2 h at 1550 °C. (a) Without any addition; (b) doped with Er; (c) doped with Eu. It must be observed that the software of the SEM automatically generates the marker length which is 1 μm in b and 2 μm in a and c. This is even if the magnification of the three photos is practically the same.

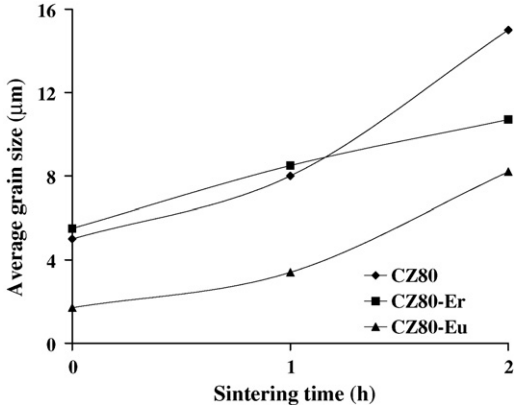

Fig. 5. Grain size vs. sintering time at 1550 °C for the three solid solutions CZ80.

which is squeezed out during the cooling process and then crystallizes in situ.

4. Conclusions

The present research demonstrates that coprecipitated and attrition milled powders of zirconia–ceria having compositions 12, 50 and 80 mole% CeO_2 can be sintered at high relative density after 2 h at 1450 °C or after 1 h at 1550 °C. Their crystal phases and microstructures can be modified by the addition of 1 mole of erbia or europia.

More in particular, microstructures of CZ12 samples doped with erbia or europia have smaller average size than pure CZ12 and it appears that erbia and europia are very effective grain growth inhibitors of these compositions. A similar behaviour we observed in the CZ80 serie which showed the cubic fluorite-type structure for any sintering cycle, but the addition of europia reduces the grain size with respect to the pure CZ80 and to the erbia-doped solution.

Pure CZ50 solid solution showed the presence of two tetragonal phases (TZ′ and TZ″) whereas CZ50-Er and CZ50-Eu show the presence of two phases if sintered at 1450 °C, but only one if fired at 1550 °C. The grains of CZ 50 and CZ50-Er have wavy borders and faceting, whereas those of CZ50-Eu have rounded borders and faceting is not greatly displayed. Both CZ50-Er and CZ80-Er microstructures show a second phase at the grain junction triple-points. This phase has not been identified, but it is thought to contribute to the smaller grain size in these samples as a result of grain pinning.

References

[1] M. Pijolat, M. Prin, M. Soustelle, O. Touret, P. Nortier, Thermal stability of doped ceria—Experimental and modelling, J. Chem. Soc. Faraday Trans. 91 (2) (1995) 3941–3948.

[2] A. Trovarelli, F. Zamar, J. Llorca, C. de Leitemburg, G. Dolcetti, J.T. Kiss, Nanophase fluorite-structured CeO_2-ZrO_2 catalysts prepared by high-energy mechanical milling—analysis of low temperature redox acivity and oxygen storage capacity, J. Catal. 169 (2) (1997) 490–502.

[3] P. Fornasiero, R. Di Monte, J.R. Rao, J. Kaspar, A. Trovarelli, M. Graziani, Rh-loaded CeO_2-ZrO_2 solid solutions as highly efficient oxygen exchangers—Dependence of the reduction behavior and oxygen storage capacity on the structural properties, J. Catal. 151 (1) (1995) 168–177.

[4] P. Fornasiero, J. Kaspar, M. Graziani, Redox behaviour of high surface area Pd-loaded $Ce_{0.5}Zr_{0.5}O_2$ mixed oxide, J. Catal. 167 (2) (1997) 576–580.

[5] P. Fornasiero, G. Balducci, R. Di Monte, J. Kaspar, V. Sergo, G. Gubitosa, A. Ferrero, M. Graziani, Modification of the redox behaviour of CeO_2 induced by structural doping with ZrO_2, J. Catal. 164 (1) (1996) 173–183.

[6] P. Vidmar, P. Fornasiero, J. Kaspar, G. Gubitosa, M. Graziani, Effects of trivalent dopants on the redox properties of $Ce_{0.6}Zr_{0.4}O_2$ mixed oxide, J. Catal. 171 (1) (1997) 160–168.

[7] F. Zamar, A. Trovarelli, C. de Leitemburg, G. Dolcetti, CeO_2-based solid solutions with the fluorite structure as novel and effective catalysts for methane combustion, J. Chem. Soc. Chem. Commun. 9 (1995) 965–966.

[8] C. de Leitemburg, A. Trovarelli, F. Zamar, S. Maschio, G. Dolcetti, J. Llorca, A novel and simple route to catalysts with high oxygen storage capacity: the direct room-temperature synthesis of CeO_2-ZrO_2 solid solutions, J. Chem. Soc. Chem. Commun. 5 (1995) 2181–2182.

[9] E. Tani, M. Yoshimura, S. Somiya, Revised phase diagram of the system ZrO_2-CeO_2 below 1400 °C, J. Am. Ceram. Soc. 66 (7) (1983) 506–510.

[10] S. Meriani, G. Spinolo, Powder data for metastable $Zr_xCe_{1-x}O_2$ (x = 0.84 to 0.40) solid solutions with tetragonal symmetry, Powder Diffr. 2 (4) (1987) 225–228.

[11] S. Maschio, O. Sbaizero, S. Meriani, Mechanical properties in the ceria-zirconia system, J. Euro. Ceram. Soc. 9 (1992) 127–132.

[12] K. Tsukuma, M. Shimada, Strength, fracture toughness and vickers hardness of CeO_2-stabilized tetragonal ZrO_2 polycrystals (Ce-TZP), J. Mater. Sci. 20 (1985) 1170–1184.

[13] L.R.F. Rose, M.V. Swain, Transformation zone shape in ceria-partially-stabilized zirconia, Acta Metall. 36 (4) (1988) 955–962.

[14] M.V. Swain, Shape memory behaviour in partially stabilized zirconia ceramics, Nature 332 (1986) 234–237.

[15] M. Watanabe, S. Iio, I. Fukuura, Aging behaviour of Y-TZP, in: N. Claussen, M. Rühle, A.H. Heuer (Eds.), Advances in Ceramics, Vol. 12 Science and Technology of Zirconia II, American Ceramic Society, Columbus, OH, 1984, pp. 391–398.

[16] T. Sato, M. Shimada, Transformation of ceria-doped tetragonal zirconia polycrystals by annealing in water, Bull. Am. Ceram. Soc. 64 (10) (1985) 1382–1384.

[17] E.R. Andrievskaya, L.M. Lopato, Influence of composition on the T → M transformation in the system ZrO_2-Ln_2O_3 (Ln = La, Nd, Sm, Eu), J. Mater. Sci. 30 (1995) 2591–2596.

[18] G. Pretorius, A stabilization mechanism of M_2O_3 c-type rare earth tetragonal stabilized ZrO_2 via co-decomposition, J. Mater. Sci. 30 (1995) 720–723.

[19] B. Bastide, P. Odier, J.P. Coutures, Phase equilibrium and martensitic transformation in lanthana-doped zirconia, J. Am. Ceram. Soc. 71 (6) (1988) 449–453.

[20] S. Maschio, S. Bruckner, G. Pezzotti, Synthesis and sintering of zirconia-erbia tetragonal solid solutions, J. Ceram. Soc. Jpn. 107 (11) (1999) 1111–1114.

[21] B. Linda, S. Maschio, S. Bruckner, G. Pezzotti, Synthesis, sintering and tetragonality of chemically derived Eu_2O_3-ZrO_2 tetragonal solid solutions, J. Ceram. Soc. Jpn. 108 (6) (2000) 593–597.

[22] M. Yashima, T. Ishizawa, M. Noma, Yoshimura, Stable and metastable phase relationships in the system ZrO_2-$ErO_{1.5}$, J. Am. Ceram. Soc. 74 (3) (1991) 510–513.

[23] P. Duran, The system erbia–zirconia, J. Am. Ceram. Soc. 60 (11–12) (1977) 510–513.

[24] W.C. Hsieh, C.S. Su, UV induced thermoluminescence in ZrO_2 doped by Er_2O_3, J. Phys. D Appl. Phys. 27 (1994) 1763–1768.

[25] K.A. Khor, J. Yang, Lattice parameters, tetragonality (c/a) and transformability of tetragonal zirconia phase in plasma-spayed ZrO_2-Er_2O_3 coatings, Mater. Lett. 31 (1997) 23–27.

[26] S. Meriani, Features of the ceria–zirconia system, Mater. Sci. Eng. A 109 (1988) 121–130.

[27] R.D. Shannon, C.T. Prewitt, Effective ionic radii in oxides and fluorides, Acta Cryst. B25 (1969) 925–1048.

[28] Bi-Shiu. Chiu, W.Y. Hsu, J.G. Duh, Dehydration of synthesized calcia-stabilized zirconia from a coprecipitation process, J. Mater. Sci. Lett. 5 (1986) 931–934.

[29] S. Maschio, A. Piras, C. Schmid, E. Lucchini, Effects of attrition milling on precursors of Al_2O_3 and 12Ce-TZP powders, J. Eur. Ceram. Soc. 21 (5) (2001) 589–594.

[30] R. Jenkins, R. Snyder, Introduction to X-ray Powder Diffractometry, Wiley, New York, 1996, p. 90.

[31] R.A. Young, The Rietveld Method, IUCr, Oxford University Press, New York, 1993.

[32] A.C. Larson, R.B. Von Dreele, General Structure Analysis System (GSAS), Los Alamos National Laboratory Report LAUR 2000, pp. 86–748.

[33] B.H. Toby, EXPGUI, a graphical user interface for GSAS, J. Appl. Cryst. 34 (2001) 210.

[34] D.J. Kim, Lattice parameters, ionic conductivities, and solubility limits in fluorite-structure MO_2 oxide (M = Hf^{4+}, Zr^{4+}, Ce^{4+}, Th^{4+}, U^{4+}), J. Am. Ceram. Soc. 72 (8) (1989) 1415.

[35] S. Meriani, Metastable tetragonal CeO_2-ZrO_2 solid solution, J. Appl. Phys. C: Suppl. 47 (2) (1986) C1485–C1489.

[36] M. Yashima, K. Morimoto, N. Ishizawa, M. Yoshimura, Zirconia-ceria solid solution synthesis and the temperature-time-transformation diagram for the 1:1 composition, J. Am. Ceram. Soc. 76 (7) (1993) 1745–1750.
[37] M. Yashima, K. Morimoto, N. Ishizawa, M. Yoshimura, Diffusionless tetragonal-cubic transformation temperature in zirconia-ceria solid solutions, J. Am. Ceram. Soc. 76 (11) (1993) 2865–2868.
[38] M. Yashima, K. Morimoto, N. Ishizawa, M. Yoshimura, Raman scattering study of cubic-tetragonal phase transition in $Zr_{1-x}Ce_xO_2$ solid solution, J. Am. Ceram. Soc. 77 (4) (1994) 1067–1071.
[39] A. Trovarelli, Structural properties and nonstoichiometric behavior of CeO_2, in: Trovarelli (Ed.), Catalysis by Ceria and Related Materials, Catalytic Science Serie, vol. 2, Imperial College Press, 2002, pp. 15–50.